Saudi Pharmaceutical Journal 25 (2017) 1047–1054

Contents lists available at ScienceDirect

Saudi Pharmaceutical Journal

journal homepage: www.sciencedirect.com

Original article

Synthesis and anticancer activity of new quinazoline derivatives

Hatem A. Abuelizz [a], Mohamed Marzouk [b,c], Hazem Ghabbour [a], Rashad Al-Salahi [a,*]

[a] Department of Pharmaceutical Chemistry, College of Pharmacy, King Saud University, P.O. Box 2457, Riyadh 11451, Saudi Arabia
[b] Department of Chemistry, College of Science and Humanities, Prince Sattam Bin Abdulaziz University, 83 Al-Kharj, Saudi Arabia
[c] Chemistry of Natural Products Group, Center of Excellence for Advanced Sciences, National Research Centre, Dokki, Cairo 12622, Egypt

ARTICLE INFO

Article history:
Received 22 February 2017
Accepted 20 April 2017
Available online 22 April 2017

Keywords:
Quinazolines
Alkylation
Hydrazinolysis
HeLa
MDA-MB231
Gefitinib
Cytotoxicity

ABSTRACT

In this study, a new series of quinazoline derivatives (**3**–**26**) was synthesized and characterized via physicochemical and spectral means. Treatment of 2-amino-5-methylbenzoic acid with butyl isothiocyanate resulted in the new 2-thioxoquinazolin-4-one (**3**). Alkylation and hydrazinolysis of the inherent thioxo group in (**1**–**3**) afforded the corresponding thioethers (**4**–**23**) and hydrazine derivatives (**24** and **25**), then **24** was further transformed into tricyclic derivative **26** via cyclocondensation reaction. Compounds **1** and **2,** which were previously synthesized, were found to exhibit anticancer activity. The cytotoxicity of all compounds was evaluated *in vitro* against the HeLa and MDA-MB231 cancer cell lines, including **1** and **2** for comparison, using MTT assay. The treatment of the cells was performed with the synthesized compounds and gefitinib at 0, 1, 5, 10, 25, and 50 μM and incubated for 24 h in 50% DMSO. The IC_{50} values of the target compounds were reported in μM, using gefitinib as a standard. Our results indicated that all compounds exhibited significant *in vitro* cytotoxicity against both cell lines. While compounds **1**–**3** showed good activity, compounds **21**–**23** were found to be more potent than gefitinib. Thus, compounds **21**–**23** may be potential anticancer agents, with IC_{50} values ranging from 1.85 to 2.81 μM in relation to gefitinib (IC_{50} = 4.3 and 28.3 μM against HeLa and MDA-MB231 cells, respectively).

1. Introduction

Although several chemotherapeutic agents are currently being used to treat human cancers, either alone or in combination, they have limited effectiveness and the response rates remain largely unimproved in clinical trials (Chandregowda et al., 2009; El-Messery et al., 2016). Despite major advances in chemotherapeutic management and cancer biology, cancer still poses a serious threat to human health globally (Al-Salahi et al., 2014a, 2015). Moreover, the great similarity between tumor and normal cells and diversity of tumor types are the main hurdles preventing the development of an ultimate anticancer therapy (El-Messery et al., 2012). Thus, persistent commitment to the arduous task of discovering and designing new anticancer agents remains critically essential.

The epidermal growth factor receptor (EGFR) plays a vital role in cell growth regulation and is considered one of the most intensely studied targets of tyrosine kinase (TK) inhibitors (El-Azab et al., 2010; Tiwari et al., 2015). Several TKs play important roles in cell proliferation, differentiation, metastasis and survival, and their unregulated activation through mechanisms such as point mutations can lead to a large percentage of clinical cancers (El-Azab et al., 2010; Tiwari et al., 2015; Al-Suwaidan et al., 2016). EGFR is overexpressed in numerous tumors, including brain, lung, bladder, ovarian, colon, breast, head, and prostate tumors (Fricker, 2006; Garofalo et al., 2008; Tiwari et al., 2015; Al-Suwaidan et al., 2016). Moreover, EGFR hyperactivation or aberrations in TKs have been implicated in other diseases including polycystic kidney disease, psoriasis, asthma, and diabetes.

Members of the erbB family of EGFR-TKs, which include erbB2 (HER2), erbB3 (HER3), and erbB4 (HER4), are overexpressed in a significant proportion of human tumors, and this overexpression is associated with poor prognosis of the disease (Meert et al., 2003; Ang et al., 2004; Chandregowda et al., 2009). Thus, inhibitors of erbB1 and erbB2 have been identified as potential anticancer drugs (Hynes and Lane, 2005; Chandregowda et al., 2009).

Of several candidate compounds that have been synthesized and tested, gefitinib (Fig. 1a) is the most potent and selective EGFR-TK inhibitor reported to date that, along with erlotinib

* Corresponding author.
E-mail address: salahi76@yahoo.com (R. Al-Salahi).
Peer review under responsibility of King Saud University.

Production and hosting by Elsevier

http://dx.doi.org/10.1016/j.jsps.2017.04.022
1319-0164/

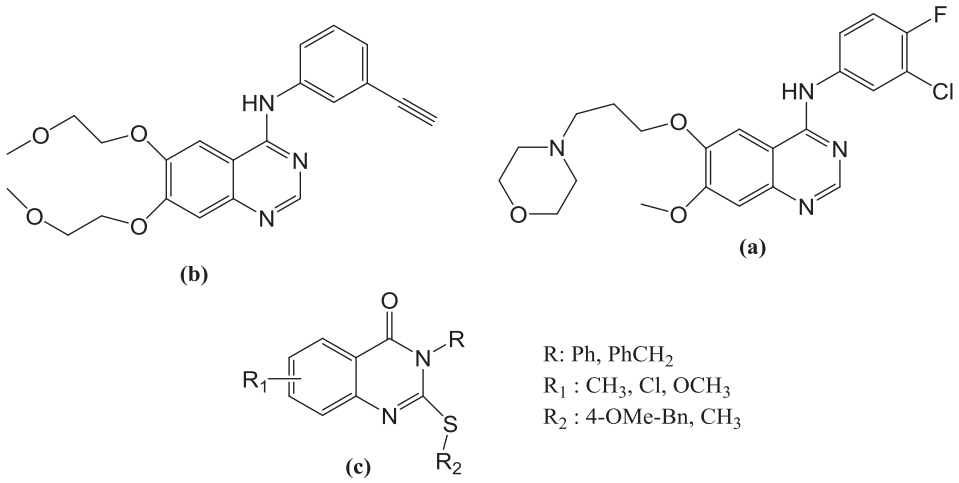

Fig. 1. Chemical structure of gefitinib, erlotinib, and quinazolines.

(Fig. 1b), has been approved by the United States Food and Drug Administration (US FDA) for the treatment of non-small cell lung cancer (NSCLC) (Arteaga and Johnson, 2001; Barker et al., 2001; Barlési et al., 2005). Gefitinib, which belongs to a new class of quinazolines, inhibits EGFR-TK overexpression through its effect on EGFR autophosphorylation and EGF-stimulated signal transduction. Hence, designing compounds with EGFR-TK inhibitory activity is an attractive chemotherapeutic strategy against malignant and nonmalignant epithelial diseases. Recently somatic mutations in the TK domain of erbB1 have been observed in a subgroup of gefitinib- and erlotinib-treated NSCLC patients (Lynch et al., 2004; Fukui et al., 2010). The focus is now on developing molecules with multiple kinase inhibition, particularly erbB1 and erbB2 inhibition (Barker and Johnstone, 1997).

Owing to the current interest on quinazolines (Fig. 1c) as antitumor agents (Al-Rashood et al., 2006; Alafeefy et al., 2014, 2015; El-Messery et al., 2016) and our ongoing studies on the quinazoline scaffold that are aimed at finding new leads with potential cytotoxic effects, we synthesized several new quinazoline derivatives (**3**–**16**, **24,** and **26**) containing a butyl group with different fragments and evaluated their *in vitro* cytotoxicity against HeLa and MDA-MB231 cancer cells. Additionally, we synthesized some derivatives (**17**–**23** and **25**) containing a benzyl group from the previously prepared parent compounds (**1**and **2**). In the present study, various functional groups were specifically incorporated at positions 3, 6, and 8 of the quinazoline scaffold to investigate the effect of various electronic environments on the cytotoxicity of the target molecules.

2. Materials and methods

2.1. Chemistry

The NMR spectra were measured on a Bruker AMX 500 spectrometer (Bruker, Billerica, MA, USA) in deuterated dimethyl sulfoxide (DMSO-d_6) and reported as δ (ppm) values relative to tetramethylsilane (TMS) at 500 and 125 MHz for ^{1}H and ^{13}C NMR, respectively. *J* values were recorded in Hz. The electrospray ionization mass spectrometry (ESI-MS) spectra were recorded using a Micromass Quattro micro™ triple-quadruple tandem mass spectrometer (Waters Corp., Milford, MA, USA). The X-ray data were collected on a Bruker APEX-II D8 Venture area diffractometer using graphite monochromatic Mo Kα radiation (λ = 0.71073 Å) at 100(2) K. The uncorrected melting point (mp) values were determined using a Stuart SMP10 melting point apparatus with open glass capillaries. The reactions were followed, and the product purity was checked by thin layer chromatography (TLC) on a DC-Mikrokarten Polygram® SIL G/UV$_{254}$, TLC plate (Thickness: 0.25 mm; Macherey-Nagel, Düren, Germany).

2.2. Preparation of 3-butyl-2,3-dihydro-6-methyl-2-thioxoquinazolin-4(1H)-one (*3*)

A mixture of butyl isothiocyanate (5 mmol) and 2-amino-5-methylbenzoic acid (5 mmol) in ethanol (15 mL) or *N,N*-dimethylformamide (DMF) (10 mL) was refluxed in the presence of triethylamine (Et_3N, 2.4 mmol) for 2 h. The mixture was then cooled and poured into ice/water (Al-Salahi et al., 2015). The resulting solid was filtered, washed with water, and dried. Yield: 90%; mp: 230–231 °C; ^{1}H NMR (DMSO-d_6) δ (ppm): 12.85 (s, 1H, —NH—), 7.75 (br s, 1H, H-5), 7.56 (br d, *J* = 8 Hz, 1H, H-7), 7.29 (d, *J* = 8.5 Hz, 1H, H-8), 4.39 (t, *J* = 7.5 Hz, 2H, H-1′), 2.36 (s, 3H, Ar—$\underline{CH_3}$), 1.66 (quintuplet, *J* = 7.5 Hz, 2H, H-2′), 1.34 (m, 2H, H-3′), 0.93 (t, *J* = 7.5 Hz, 3H, H-4′); ^{13}C NMR (DMSO-d_6) δ (ppm): 174.9 (C-2), 159.7 (C-4), 137.5 (C-4b), 136.9 (C-6), 134.5 (C-7), 127.0 (C-5), 116.0 (C-8), 115.8 (C-4a), 45.9 (C-1′), 28.9 (C-2′), 20.9 (Ar—$\underline{CH_3}$), 20.1 (C-3′), 14.2 (C-4′); ESI-MS (*m*/*z*): 247.3 $[M-H]^-$ (negative mode) for molecular weight (MW) = 248.34.

2.3. General procedure for the Preparation of compounds *4*–*23*

Potassium carbonate (1.2 mmol) was added portion-wise over a period of 5 min to a mixture of compounds **1**, **2** or **3** (1 mmol) in DMF (8 mL) at room temperature. The appropriate alkyl halide (1.5 mmol) was then added, and the reaction mixture was stirred at 90 °C for 18 h. The mixture was poured into ice/water, and the precipitate was filtered off, washed with water, and dried (Al-Salahi et al., 2015).

2.3.1. 3-Butyl-2-(ethylthio)-6-methylquinazolin-4(3H)-one (*4*)

White amorphous powder; yield: 77%; mp: 89–90 °C; ^{1}H NMR (DMSO-d_6) δ (ppm): 7.86 (br s, 1H, H-5), 7.59 (br d, *J* = 8 Hz, 1H, H-7), 7.44 (d, *J* = 8.5 Hz, 1H, H-8), 4.02 (t, *J* = 7.5 Hz, 2H, H-1″), 3.26 (q, *J* = 7.5 Hz, 2H, H-1′), 2.42 (s, 3H, Ar—CH_3), 1.65 (quintuplet, *J* = 7.5 Hz, 2H, H-2″), 1.37 (m, 5H, H-2′, H-3″), 0.93 (t, *J* = 7.5 Hz, 3H, H-4″); ^{13}C NMR (DMSO-d_6) δ (ppm): 160.9 (C-4), 155.8 (C-2), 145.5 (C-4b), 136.3 (C-7), 135.8 (C-6), 126.2 (C-5), 126.1 (C-8), 118.9 (C-4a), 44.1 (C-1″), 30.1 (C-2″), 26.3 (C-1′), 21.2 (Ar—CH_3), 20.1 (C-3″), 14.4 (C-2′), 14.1 (C-4″); ESI-MS (*m*/*z*): 275.4 $[M-H]^-$ (negative mode) for MW = 276.40.

*2.3.2. 2-(Allylthio)-3-butyl-6-methylquinazolin-4(3H)-one (**5**)*

Pale yellow amorphous powder; yield: 80%; mp: 67–68 °C; ^{1}H NMR (DMSO-d_6) δ (ppm): 7.86 (br s, 1H, H-5), 7.59 (br d, J = 8 Hz, 1H, H-7), 7.45 (d, J = 8.5 Hz, 1H, H-8), 6.00 (m, 1H, H-2′), 5.41 (br d, J = 17 Hz, 1H, H-3a′), 5.18 (br d, J = 10 Hz, 1H, H-3b′), 4.02 (t, J = 7.5 Hz, 2H, H-1″), 3.96 (d, J = 7 Hz, 2H, H-1′), 2.42 (s, 3H, Ar—CH_3), 1.65 (quintuplet, J = 7.5 Hz, 2H, H-2″), 1.35 (m, 2H, H-3″), 0.93 (t, J = 7.5 Hz, 3H, H-4″); ^{13}C NMR (DMSO-d_6) δ (ppm): 160.9 (C-4), 155.1 (C-2), 145.4 (C-4b), 136.3 (C-7), 135.9 (C-6), 133.4 (C-2′), 126.3 (C-5), 126.1 (C-8), 119.5 (C-3′), 119.0 (C-4a), 44.1 (C-1″), 34.5 (C-1′), 30.1 (C-2″), 21.2 (Ar—CH_3), 20.1 (C-3″), 14.0 (C-4″); ESI-MS (m/z): 287.1 [M−H]$^-$ (negative mode) for MW = 288.41.

*2.3.3. 3-Butyl-6-methyl-2-(2-methylbenzylthio)-quinazolin-4(3H)-one (**6**)*

White amorphous powder; yield: 77%; mp: 101–102 °C; ^{1}H NMR (DMSO-d_6) δ (ppm): 7.87 (br s, 1H, H-5), 7.63 (br d, J = 8 Hz, 1H, H-7), 7.53 (d, J = 8.5 Hz, 1H, H-8), 7.49 (d, J = 8.5 Hz, 1H, H-3′), 7.20–7.10 (m, 3H, H-4′,5′,6′), 4.56 (s, 2H, H-7′), 4.00 (t, J = 7.5 Hz, 2H, H-1″), 2.43 (s, 3H, —CH_2—Ar—CH_3), 2.42 (s, 3H, Ar—CH_3), 1.62 (quintuplet, J = 7.5 Hz, 2H, H-2″), 1.33 (m, 2H, H-3″), 0.90 (t, J = 7.5 Hz, 3H, H-4″); ^{13}C NMR (DMSO-d_6) δ (ppm): 160.9 (C-4), 155.5 (C-2), 145.4 (C-4b), 137.4 (C-1′), 136.4 (C-7), 136.0 (C-6), 134.4 (C-2′), 130.9 (C-3′), 130.8 (C-4′), 128.3 (C-6′), 126.5 (C-5′), 126.3 (C-5), 126.2 (C-8), 119.1 (C-4a), 44.2 (C-1″), 34.5 (C-7′), 30.1 (C-2″), 21.2 (Ar—CH_3), 20.0 (C-3″), 19.4 (—CH_2—Ar—CH_3), 14.0 (C-4″); ESI-MS (m/z): 351.1 [M−H]$^-$ (negative mode) for MW = 352.50.

*2.3.4. 3-Butyl-6-methyl-2-(3-methylbenzylthio)-quinazolin-4(3H)-one (**7**)*

Pale yellow amorphous powder; yield: 80%; mp: 84–85 °C; ^{1}H NMR (DMSO-d_6) δ (ppm): 7.87 (br s, 1H, H-5), 7.62 (br d, J = 8 Hz, 1H, H-7), 7.52 (d, J = 8.5 Hz, 1H, H-8), 7.32 (br s, 1H, H-2′), 7.30 (br d, J = 8 Hz, 1H, H-4′), 7.21 (t-like, J = 8 Hz, 1H, H-5′), 7.07 (br d, J = 8 Hz, 1H, H-6′), 4.50 (s, 2H, H-7′), 4.00 (t, J = 7.5 Hz, 2H, H-1″), 2.42 (s, 3H, Ar—CH_3), 2.28 (s, 3H, —CH_2—Ar—CH_3), 1.61 (quintuplet, J = 7.5 Hz, 2H, H-2″), 1.34 (m, 2H, H-3″), 0.92 (t, J = 7.5 Hz, 3H, H-4″); ^{13}C NMR (DMSO-d_6) δ (ppm): 160.9 (C-4), 155.4 (C-2), 145.4 (C-4b), 138.0 (C-1′), 136.9 (C-3′), 136.4 (C-7), 136.0 (C-6), 130.5 (C-5′), 128.8 (C-4′), 128.5 (C-2′), 126.9 (C-6′), 126.2 (C-5), 126.1 (C-8), 119.0 (C-4a), 44.1 (C-1″), 36.0 (C-7′), 30.1 (C-2″), 21.4 (—CH_2—Ar—CH_3), 21.2 (Ar—CH_3), 20.0 (C-3″), 14.0 (C-4″); ESI-MS (m/z): 351.1 [M−H]$^-$ (negative mode) for MW = 352.50.

*2.3.5. 3-Butyl-2-(4-chlorobenzylthio)-6-methyl-3H-quinazolin-4-one (**8**)*

White amorphous powder; yield: 70%; mp: 110–111 °C; ^{1}H NMR (DMSO-d_6) δ (ppm): 7.86 (br s, 1H, H-5), 7.63 (br d, J = 8 Hz, 1H, H-7), 7.55 (d, J = 8 Hz, 2H, H-3′/5′), 7.53 (d, J = 8.5 Hz, 1H, H-8), 7.38 (d, J = 8 Hz, 2H, H-2′/6′), 4.54 (s, 2H, H-7′), 4.01 (t, J = 7.5 Hz, 2H, H-1″), 2.43 (s, 3H, Ar—CH_3), 1.63 (quintuplet, J = 7.5 Hz, 2H, H-2″), 1.33 (m, 2H, H-3″), 0.91 (t, J = 7.5 Hz, 3H, H-4″); ^{13}C NMR (DMSO-d_6) δ (ppm): 160.9 (C-4), 155.1 (C-2), 145.3 (C-4b), 136.7 (C-4′), 136.4 (C-7), 136.1 (C-6), 132.4 (C-1′), 131.7 (C-3′/5′), 128.8 (C-2′/6′), 126.3 (C-5), 126.2 (C-8), 119.0 (C-4a), 44.2 (C-1″), 35.0 (C-7′), 30.1 (C-2″), 21.2 (Ar—CH_3), 20.0 (C-3″), 14.0 (C-4″); ESI-MS (m/z): 371.0 [M−H]$^-$ (negative mode) for MW = 372.91.

*2.3.6. 3-butyl-6-methyl-2-(4-Nitrobenzylthio)quinazolin-4(3H)-one (**9**)*

White amorphous powder; yield: 82%; mp: 146–147 °C; ^{1}H NMR (DMSO-d_6) δ (ppm): 8.18 (d, J = 8 Hz, 2H, H-3′/5′), 7.85 (br s, 1H, H-5), 7.82 (d, J = 8 Hz, 2H, H-2′/6′), 7.63 (br d, J = 8 Hz, 1H, H-7), 7.55 (d, J = 8.5 Hz, 1H, H-8), 4.67 (s, 2H, H-7′), 4.02 (t, J = 7.5 Hz, 2H, H-1″), 2.42 (s, 3H, Ar—CH_3), 1.66 (quintuplet, J = 7.5 Hz, 2H, H-2″), 1.35 (m, 2H, H-3″), 0.92 (t, J = 7.5 Hz, 3H, H-4″); ^{13}C NMR (DMSO-d_6) δ (ppm): 160.9 (C-4), 155.2 (C-2), 147.1 (C-4′), 146.2 (C-1′), 145.2 (C-4b), 136.4 (C-7), 136.2 (C-6), 131.7 (C-2′/6′), 126.3 (C-5), 126.2 (C-8), 123.9 (C-3′/5′), 119.1 (C-4a), 44.2 (C-1″), 34.9 (C-7′), 30.1 (C-2″), 21.2 (Ar—CH_3), 20.0 (C-3″), 14.0 (C-4″); ESI-MS (m/z): 382.1 [M−H]$^-$ (negative mode) for MW = 383.47.

*2.3.7. 2-[(3-Butyl-3,4-dihydro-6-methyl-4-oxoquinazolin-2-ylthio) methyl]benzo nitrile (**10**)*

White amorphous powder; yield: 76%; mp: 128–129 °C; ^{1}H NMR (DMSO-d_6) δ (ppm): 7.85 (br s, 1H, H-5), 7.82 (br d, J = 8 Hz, 1H, H-6′), 7.67 (t-like, J = 8 Hz, 1H, H-5′), 7.62 (br d, J = 8 Hz, 1H, H-7), 7.60 (br d, J = 8 Hz, 1H, H-3′), 7.56 (d, J = 8.5 Hz, 1H, H-8), 7.46 (t-like, 1H, H-4′) 4.70 (s, 2H, H-7′), 4.01 (t, J = 7.5 Hz, 2H, H-1″), 2.41 (s, 3H, Ar—CH_3), 1.64 (quintuplet, J = 7.5 Hz, 2H, H-2″), 1.35 (m, 2H, H-3″), 0.91 (t, J = 7.5 Hz, 3H, H-4″); ^{13}C NMR (DMSO-d_6) δ (ppm): 160.8 (C-4), 154.5 (C-2), 145.3 (C-4b), 141.4 (C-1′), 136.4 (C-7), 136.2 (C-6), 133.7 (C-5′), 133.4 (C-3′), 131.1 (C-6′), 128.7 (C-4′), 126.2 (C-5), 126.1 (C-8), 119.1 (C-4a), 118.2 (—CN), 112.8 (C-2′), 44.2 (C-1″), 34.1 (C-7′), 30.1 (C-2″), 21.2 (Ar—CH_3), 20.0 (C-3″), 14.0 (C-4″); ESI-MS (m/z): 362.0 [M−H]$^-$ (negative mode) for MW = 363.48.

*2.3.8. 3-[(3-Butyl-3,4-dihydro-6-methyl-4-oxoquinazolin-2-ylthio) methyl]benzo nitrile (**11**)*

White amorphous powder; yield: 71%; mp: 139–140 °C; ^{1}H NMR (DMSO-d_6) δ (ppm): 8.02 (br s, 1H, H-2′), 7.88 (br d, J = 8 Hz, 1H, H-6′), 7.86 (br s, 1H, H-5), 7.63 (br d, J = 8 Hz, 1H, H-7), 7.56 (d, J = 8.5 Hz, 1H, H-8), 7.54 (m, 2H, H-4′,5′), 4.58 (s, 2H, H-7′), 4.01 (t, J = 7.5 Hz, 2H, H-1″), 2.42 (s, 3H, Ar—CH_3), 1.63 (quintuplet, J = 7.5 Hz, 2H, H-2″), 1.34 (m, 2H, H-3″), 0.91 (t, J = 7.5 Hz, 3H, H-4″); ^{13}C NMR (DMSO-d_6) δ (ppm): 160.9 (C-4), 154.9 (C-2), 145.2 (C-4b), 139.8 (C-1′), 136.5 (C-7), 136.2 (C-6), 134.8 (C-6′), 133.5 (C-2′), 131.5 (C-4′), 130.0 (C-5′), 126.2 (C-5), 126.1 (C-8), 119.1 (C-4a), 119.0 (—CN), 111.7 (C-3′), 44.2 (C-1″), 34.8 (C-7′), 30.1 (C-2″), 21.2 (Ar—CH_3), 20.0 (C-3″), 14.0 (C-4″); ESI-MS (m/z): 362.0 [M−H]$^-$ (negative mode) for MW = 363.48.

*2.3.9. 4-[(3-Butyl-3,4-dihydro-6-methyl-4-oxoquinazolin-2-ylthio) methyl]benzo nitrile (**12**)*

White amorphous powder; yield: 78%; mp: 124–125 °C; ^{1}H NMR (DMSO-d_6) δ (ppm): 7.85 (br s, 1H, H-5), 7.79 (d, J = 8 Hz, 2H, H-3′/5′), 7.73 (d, J = 8 Hz, 2H, H-2′/6′), 7.62 (br d, J = 8 Hz, 1H, H-7), 7.52 (d, J = 8.5 Hz, 1H, H-8), 4.61 (s, 2H, H-7′), 4.00 (t, J = 7.5 Hz, 2H, H-1″), 2.42 (s, 3H, Ar—CH_3), 1.62 (quintuplet, J = 7.5 Hz, 2H, H-2″), 1.34 (m, 2H, H-3″), 0.91 (t, J = 7.5 Hz, 3H, H-4″); ^{13}C NMR (DMSO-d_6) δ (ppm): 160.9 (C-4), 154.9 (C-2), 145.2 (C-4b), 143.9 (C-1′), 136.4 (C-7), 136.2 (C-6), 132.7 (C-3′/5′), 130.8 (C-2′/6′), 126.2 (C-5), 126.1 (C-8), 119.2 (C-4a), 119.0 (—CN), 110.5 (C-4′), 44.2 (C-1″), 35.2 (C-7′), 30.1 (C-2″), 21.2 (Ar—CH_3), 20.0 (C-3″), 14.0 (C-4″); ESI-MS (m/z): 362.0 [M−H]$^-$ (negative mode) for MW = 363.48.

*2.3.10. 3-Butyl-6-methyl-2-(3-methoxybenzylthio)-quinazolin-4(3H)-one (**13**)*

White amorphous powder; yield: 80%; mp: 83–84 °C; ^{1}H NMR (DMSO-d_6) δ (ppm): 7.87 (br s, 1H, H-5), 7.61 (br d, J = 8 Hz, 1H, H-7), 7.53 (d, J = 8.5 Hz, 1H, H-8), 7.24 (t-like, J = 8 Hz, 1H, H-5′), 7.11 (br s, 1H, H-2′), 7.08 (br d, J = 8 Hz, 1H, H-4′), 6.83 (br d, J = 8 Hz, 1H, H-6′), 4.51 (s, 2H, H-7′), 4.01 (t, J = 7.5 Hz, 2H, H-1″), 3.73 (s, 3H, —OCH_3), 2.43 (s, 3H, Ar—CH_3), 1.63 (quintuplet, J = 7.5 Hz, 2H, H-2″), 1.33 (m, 2H, H-3″), 0.90 (t, J = 7.5 Hz, 3H, H-4″); ^{13}C NMR (DMSO-d_6) δ (ppm): 160.9 (C-4), 159.7 (C-3′), 155.4

(C-2), 145.3 (C-4b), 138.8 (C-1′), 136.4 (C-7), 136.0 (C-6), 130.0 (C-5′), 126.2 (C-5), 126.1 (C-8), 122.0 (C-6′), 119.0 (C-4a), 115.4 (C-4′), 113.4 (C-2′), 55.5 (—OCH_3), 44.1 (C-1″), 35.9 (C-7′), 30.1 (C-2″), 21.2 (Ar—CH_3), 20.0 (C-3″), 14.0 (C-4″); ESI-MS (*m*/*z*): 367.3 $[M-H]^-$ (negative mode) for MW = 368.50.

*2.3.11. 2-[(1H-benzo[d]imidazol-2-yl)methylthio]-3-butyl-6-methylquinazolin-4(3H)-one (**14**)*

Brown amorphous powder; yield: 45%; mp: 114–115 °C; ^{1}H NMR (DMSO-d_6) δ (ppm): 12.45 (br s, 1H, NH), 7.87 (br s, 1H, H-5), 7.61 (br d, *J* = 8 Hz, 1H, H-7), 7.56 (d, *J* = 8.5 Hz, 1H, H-8), 7.16 (m, 4H, H-4′, 5′, 6′, 7′-benzimidazole), 4.80 (s, 2H, —CH_2—), 4.06 (t, *J* = 7.5 Hz, 2H, H-1″), 2.42 (s, 3H, Ar—CH_3), 1.68 (quintuplet, *J* = 7.5 Hz, 2H, H-2″), 1.36 (m, 2H, H-3″), 0.93 (t, *J* = 7.5 Hz, 3H, H-4″); ^{13}C NMR (DMSO-d_6) δ (ppm): 160.9 (C-4), 154.9 (C-2), 150.3 (C-2′), 145.3 (C-4b), 136.9 (C-3′a, 7′a), 136.4 (C-7), 136.2 (C-6), 127.0 (C-5′, 6′), 126.4 (C-5), 126.1 (C-8), 119.1 (C-4a), 116.0 (C-4′, 7′), 44.3 (C-1″), 30.1 (C-2″), 28.9 (—CH_2—), 21.2 (Ar—CH_3), 20.1 (C-3″), 14.0 (C-4″); ESI-MS (*m*/*z*): 377.0 $[M-H]^-$ (negative mode) for MW = 378.49.

*2.3.12. 3-butyl-6-methyl-2-(2-Morpholinoethylthio)quinazolin-4 (3H)-one (**15**)*

Pale brown amorphous powder; yield: 60%. mp: 201–202 °C; ^{1}H NMR (DMSO-d_6) δ (ppm): 7.86 (br s, 1H, H-5), 7.60 (br d, *J* = 8 Hz, 1H, H-7), 7.56 (d, *J* = 8.5 Hz, 1H, H-8), 4.04 (t, *J* = 7.5 Hz, 2H, H-1″), 3.56 (t, *J* = 4.0 Hz, 4H, H-3′/5′), 3.40 (t, *J* = 7.5 Hz, 2H, CH_2-7′), 2.67 (t, *J* = 7.5 Hz, 2H, CH_2-8′), 2.47 (t, *J* = 4.0 Hz, 4H, H-2′/6′), 2.42 (s, 3H, Ar—CH_3), 1.67 (quintuplet, *J* = 7.5 Hz, 2H, H-2″), 1.37 (m, 2H, H-3″), 0.93 (t, *J* = 7.5 Hz, 3H, H-4″); ^{13}C NMR (DMSO-d_6) δ (ppm): 159.7 (C-4), 155.9 (C-2), 145.4 (C-4b), 136.9 (C-7), 136.4 (C-6), 126.2 (C-5), 126.1 (C-8), 118.9 (C-4a), 66.7 (C-3′/5′), 57.4 (CH_2-7′), 53.5 (C-2′/6′), 44.1 (C-1″), 30.1 (C-2″), 29.0 (CH_2-8′), 21.2 (Ar—CH_3), 20.1 (C-3″), 14.2 (C-4″); ESI-MS (*m*/*z*): 360.2 $[M-H]^-$ (negative mode) for MW = 361.50.

*2.3.13. 2-[3-(3-Butyl-3,4-dihydro-6-methyl-4-oxoquinazolin-2-ylthio)propyl]isoindo line-1,3-dione (**16**)*

White amorphous powder; yield: 80%; mp: 105–106 °C; ^{1}H NMR (DMSO-d_6) δ (ppm): 7.87 (m, 4H, H-5′/6′, 4′/7′), 7.81 (br s, 1H, H-5), 7.47 (br d, *J* = 8 Hz, 1H, H-7), 7.07 (d, *J* = 8.5 Hz, 1H, H-8), 3.97 (t, *J* = 7.5 Hz, 2H, H-1″), 3.74 (t, *J* = 7 Hz, 2H, CH_2-7′), 3.28 (t, *J* = 7 Hz, 2H, CH_2-9′), 2.39 (s, 3H, Ar—CH_3), 2.07 (quintuplet, *J* = 7.2 Hz, 2H, CH_2-8′), 1.62 (quintuplet, *J* = 7.5 Hz, 2H, H-2″), 1.32 (m, 2H, H-3″), 0.90 (t, *J* = 7.5 Hz, 3H, H-4″); ^{13}C NMR (DMSO-d_6) δ (ppm): 168.5 (C-1′/3′), 160.9 (C-4), 155.5 (C-2), 145.3 (C-4b), 136.2 (C-7), 135.9 (C-6), 134.9 (C-3a′/7a′), 132.2 (C-5′/6′), 126.1 (C-5), 126.0 (C-8), 123.5 (C-4′/7′), 118.9 (C-4a), 44.0 (C-1″), 37.1 (CH_2-7′), 34.6 (CH_2-9′), 30.0 (C-2″), 28.3 (CH_2-8′), 21.2 (Ar—CH_3), 20.0 (C-3″), 14.0 (C-4″); ESI-MS (*m*/*z*): 434.4 $[M-H]^-$ (negative mode) for MW = 435.54.

*2.3.14. 4-[(3-Benzyl-3,4-dihydro-6-methyl-4-oxoquinazolin-2-ylthio) methyl]benzonitrile (**17**)*

White amorphous powder; yield: 80%; mp: 174–175 °C (DMF); ^{1}H NMR (500 MHz, DMSO-d_6) δ (ppm): 7.91 (br s, 1H, H-5), 7.76 (d, *J* = 8 Hz, H-3′/5′), 7.68 (m, 3H, H-7, 2′/6′), 7.57 (d, *J* = 8 Hz, 1H, H-8), 7.32 (t-like, *J* = 7.5 Hz, 2H, H-3″/5″), 7.26 (br d, *J* = 7.5 Hz, 1H, H-4″), 7.19 (br d, *J* = 7.5 Hz, 2H, H-2″/6″), 5.30 (s, 2H, H-7″), 4.57 (s, 2H, H-7′), 2.44 (s, 3H, Ar—CH_3); ^{13}C NMR (125 MHz, DMSO-d_6) δ (ppm): 161.3 (C-4), 155.3 (C-2), 145.3 (C-4b), 143.9 (C-1′), 136.7 (C-6), 136.5 (C-1″), 136.1 (C-7), 132.7 (C-3′/5′), 130.6 (C-2′/6′), 129.0 (C-3″/5″), 127.9 (C-4″), 127.1 (C-2″/6″), 126.4 (C-5), 126.3 (C-8), 119.2 (C-4a), 118.9 (—CN), 110.4 (C-4′), 47.2 (C-7″), 35.4 (C-7′), 21.2 (Ar—CH_3); ESI-MS (*m*/*z*): 396.12 $[M-H]^-$ (negative mode) for MW = 397.50.

*2.3.15. 3-Benzyl-6-methyl-2-(3-methylbenzylthio)-quinazolin-4(3H)-one (**18**)*

White amorphous powder; yield: 70%; mp: 130–131 °C (DMF); ^{1}H NMR (500 MHz, DMSO-d_6) δ (ppm): 7.92 (d, *J* = 1.5 Hz, 1H, H-5), 7.66 (dd, *J* = 8, 1.5 Hz, 1H, H-7), 7.57 (d, *J* = 8 Hz, 1H, H-8), 7.30–7.15 (m, 8H, H-2′, 4′, 5′, 3″/5″, 4″, 2″/6″), 7.06 (br d, *J* = 7.5 Hz, 1H, H-6′), 5.30 (s, 2H, H-7″), 4.47 (s, 2H, H-7′), 2.45 (s, 3H, Ar—CH_3), 2.26 (s, 3H, —CH_2—Ar—CH_3); ^{13}C NMR (125 MHz, DMSO-d_6) δ (ppm): 161.4 (C-4), 155.9 (C-2), 145.4 (C-4b), 138.0 (C-1′), 136.8 (C-3′), 136.7 (C-6), 136.3 (C-1″), 136.2 (C-7), 130.4 (C-5′), 129.0 (C-4′), 128.9 (C-3″/5″), 128.5 (C-2′), 127.8 (C-2″/6″), 127.1 (C-6′), 126.9 (C-4″), 126.4 (C-5), 126.3 (C-8), 119.0 (C-4a), 47.1 (C-7″), 36.1 (C-7′), 21.4 (—CH_2—Ar—CH_3), 21.2 (Ar—CH_3); ESI-MS (*m*/*z*): 385.15 $[M-H]^-$ (negative mode) for MW = 386.51.

*2.3.16. 3-Benzyl-6-methyl-2-(4-nitrobenzylthio)-quinazolin-4(3H)-one (**19**)*

Yellow amorphous powder; yield: 72%; mp: 165–166 °C (DMF); ^{1}H NMR (500 MHz, DMSO-d_6) δ (ppm): 8.15 (d, *J* = 7.5 Hz, 2H, H-3′/5′), 7.94 (d, *J* = 7.5 Hz, 2H, H-2′/6′), 7.90 (br s, 1H, H-5), 7.67 (br d, *J* = 8 Hz, 1H, H-7), 7.59 (d, *J* = 8 Hz, 1H, H-8), 7.30 (t-like, *J* = 7.5 Hz, 2H, H-3″/5″), 7.21 (br d, *J* = 7.5 Hz, 1H, H-4″), 7.13 (br d, *J* = 7.5 Hz, 2H, H-2″/6″), 5.30 (s, 2H, H-7″), 4.62 (s, 2H, H-7′), 2.44 (s, 3H, Ar—CH_3); ^{13}C NMR (125 MHz, DMSO-d_6) δ (ppm): 161.1 (C-4), 155.5 (C-2), 147.1 (C-4′), 146.0 (C-4b), 145.1 (C-1′), 136.7 (C-6), 136.6 (C-1″), 136.0 (C-7), 131.0 (C-2′/6′), 129.1 (C-3″/5″), 127.9 (C-4″), 127.4 (C-2″/6″), 127.0 (C-5), 126.4 (C-8), 123.8 (C-3′/5′), 119.2 (C-4a), 47.2 (C-7″), 35.1 (C-7′), 20.7 (Ar—CH_3); ESI-MS (*m*/*z*): 416.1 $[M-H]^-$ (negative mode) for MW = 417.48.

*2.3.17. (3-Benzyl-6-methyl-2-(7-nitrobenzo[d][1,2,3]oxadiazol-4-yl) thio)quinazolin-4(3H)-one (**20**)*

Pale brown amorphous powder; yield: 54%; mp: 147–148 °C (DMF); ^{1}H NMR (500 MHz, DMSO-d_6) δ (ppm): 8.08 (d, *J* = 8 Hz, H-5′), 7.84 (br d, *J* = 8 Hz, 1H, H-5), 7.58 (br d, *J* = 8 Hz, 1H, H-7), 7.50–7.12 (m, 7H, H-6′, 3″/5″, 4″, 2″/6″, 8), 5.54 (s, 2H, H-7″), 2.44 (s, 3H, Ar—CH_3); ^{13}C NMR (125 MHz, DMSO-d_6) δ (ppm): 161.8 (C-4), 159.0 (C-2), 145.0 (C-7′), 143.9 (C-4b), 139.1 (C-4′), 136.8 (C-6), 136.1 (C-1″), 136.1 (C-7), 131.1 (C-3a′), 130.8 (C- 5′), 129.0 (C-3″/5″), 127.8 (C-4″), 127.1 (C-2″/6″), 126.3 (C-5), 126.1 (C-8), 124.2 (C-7a′), 123.5 (C-6′), 118.9 (C-4a), 47.1 (C-7″), 21.1 (Ar—CH_3); ESI-MS (*m*/*z*): 444.1 $[M-H]^-$ (negative mode) for MW = 445.45.

*2.3.18. 2-[3-((3-Benzyl-6-methyl-4-oxo-3,4-dihydroquinazolin-2-yl) thio)propyl]isoin doline-1,3-dione (**21**)*

White amorphous powder; yield: 78%; mp: 152–153 °C (DMF); ^{1}H NMR (500 MHz, DMSO-d_6) δ (ppm): 7.84 (m, 5H, H-5′/6′, 4′/7′, 5), 7.54 (dd, *J* = 8, 2 Hz, 1H, H-7), 7.32 (t-like, *J* = 7.5 Hz, 2H, H-3″/5″), 7.26 (br d, *J* = 7.5 Hz, 1H, H-4″), 7.20 (br d, *J* = 7.5 Hz, 2H, H-2″/6″), 7.12 (d, *J* = 8 Hz, 1H, H-8), 5.28 (s, 2H, H-7″), 3.71 (t, *J* = 7 Hz, 2H, CH_2-7′), 3.24 (t, *J* = 7 Hz, 2H, CH_2-9′), 2.42 (s, 3H, Ar—CH_3), 2.03 (quintuplet, *J* = 70 Hz, 2H, CH_2-8′); ^{13}C NMR (125 MHz, DMSO-d_6) δ (ppm): 168.5 (C-1′/3′), 161.3 (C-4), 155.6 (C-2), 145.4 (C-4b), 136.5 (C-6), 136.2 (C-1″), 136.1 (C-7), 134.9 (C-5′/6′), 132.2 (C-3a′/7a′), 129.0 (C-3″/5″), 127.8 (C-4″), 127.1 (C-2″/6″), 126.3 (C-5), 126.1 (C-8), 123.5 (C-4′/7′), 118.9 (C-4a), 47.1 (C-7″), 37.0 (CH_2-7′), 29.3 (CH_2-9′), 28.3 (CH_2-8′), 21.2 (Ar—CH_3); ESI-MS (*m*/*z*): 468.01 $[M-H]^-$ (negative mode) for MW = 469.56.

*2.3.19. 2-[3-((3-Benzyl-8-methoxy-4-oxo-3,4-dihydroquinazolin-2-yl) thio)propyl] isoindoline-1,3-dione (**22**)*

Pale brown amorphous powder; yield: 85%; mp: 145–1146 °C (DMF); ^{1}H NMR (500 MHz, DMSO-d_6) δ (ppm): 7.82 (m, 4H, H-5′/6′, 4′/7′), 7.64 (br d, *J* = 8 Hz, 1H, H-5), 7.38 (t-like, *J* = 8 Hz, 1H, H-6), 7.34 (br d, *J* = 8 Hz, 1H, H-7), 7.31 (t-like, *J* = 7.5 Hz, 2H, H-3″/5″), 7.27 (br d, *J* = 7.5 Hz, 1H, H-4″), 7.23 (br d, *J* = 7.5 Hz, 2H,

H-2″/6″), 5.30 (s, 2H, H-7″), 3.79 (s, 3H, —OCH_3), 3.72 (t, J = 7 Hz, 2H, CH_2-7′), 3.31 (t, J = 7 Hz, 2H, CH_2-9′), 2.08 (quintuplet, J = 70 Hz, 2H, CH_2-8′); ^{13}C NMR (125 MHz, DMSO-d_6) δ (ppm): 168.4 (C-1′/3′), 161.4 (C-4), 155.7 (C-2), 153.9 (C-8), 138.0 (C-4b), 136.1 (C-1″), 134.8 (C-5′/6′), 132.1 (C-3a′/7a′), 129.0 (C-3″/5″), 127.8 (C-6), 127.1 (C-2″/6″), 126.7 (C-4″), 123.4 (C-4′/7′), 120.1 (C-4a), 117.9 (C-7), 116.1 (C-5), 56.7 (—OCH_3), 47.3 (C-7″), 37.0 (CH_2-7′), 29.6 (CH_2-9′), 28.1 (CH_2-8′); ESI-MS (m/z): 484.1 [M−H]$^-$ (negative mode) for MW = 485.56.

*2.3.20. 3-Benzyl-8-methoxy-2-((2-morpholinoethyl)thio)quinazolin-4 (3H)-one (**23**)*

Pale yellow amorphous powder; yield: 65%; mp: 129–130 °C (DMF); ^{1}H NMR (500 MHz, DMSO-d_6) δ (ppm): 7.52 (br d, J = 8 Hz, 1H, H-5), 7.41–7.37 (m, 2H, H-6, 7), 7.31 (t-like, J = 7.5 Hz, 2H, H-3″/5″), 7.26 (br d, J = 7.5 Hz, 1H, H-4″), 7.22 (br d, J = 7.5 Hz, 2H, H-2″/6″), 5.32 (s, 2H, H-7″), 3.89 (s, 3H, —OCH_3), 3.53 (t, J = 4.0 Hz, 4H, H-3′/5′), 3.40 (t, J = 7 Hz, 2H, CH_2-7′), 2.64 (t, J = 7 Hz, 2H, CH_2-8′), 2.47 (t, J = 4.0 Hz, 4H, H-2′/6′); ^{13}C NMR (125 MHz, DMSO-d_6) δ (ppm): 161.4 (C-4), 156.0 (C-2), 153.9 (C-8), 138.1 (C-4b), 136.2 (C-1″), 129.0 (C-3″/5″), 127.8 (C-6), 127.1 (C-2″/6″), 126.7 (C-4″), 120.1 (C-4a), 117.9 (C-7), 116.5 (C-5), 66.7 (C-3′/5′), 57.5 (CH_2-7′), 56.6 (C—OCH_3), 53.5 (C-2′/6′), 47.3 (C-7″), 29.0 (CH_2-8′); ESI-MS (m/z): 410.1 [M−H]$^-$ (negative mode) for MW = 411.52.

*2.4. Preparation of 2-hydrazinyl-6-methyl-3H-quinazolin-4-ones (**24** and **25**)*

Compound **1** or **3** (1 mmol) was boiled with hydrazine hydrate (5 mmol) in ethanol (10 mL) for 7 h under reflux. The mixture was cooled, and the precipitate was filtered, washed with water and dried.

*2.4.1. 3-Butyl-2-hydrazinyl-6-methyl-3H-quinazolin-4-one (**24**)*

White amorphous powder; yield: 76%; mp: 177–178 °C; ^{1}H NMR (DMSO-d_6) δ (ppm): 9.44 (s, 1H, —NH—), 8.08 (d, J = 8.5 Hz, 1H, H-8), 7.97 (br s, 1H, H-5), 7.73 (br d, J = 8 Hz, 1H, H-7), 6.21 (br s, 2H, —NH_2), 4.17 (t, J = 7.5 Hz, 2H, H-1′), 2.45 (s, 3H, Ar—CH_3), 1.74 (quintuplet, J = 7.5 Hz, 2H, H-2′), 1.37 (m, 2H, H-3′), 0.92 (t, J = 7.5 Hz, 3H, H-4′); ^{13}C NMR (DMSO-d_6) δ (ppm): 158.6 (C-4), 147.8 (C-2), 137.0 (C-4b), 136.2 (C-7), 130.9 (C-6), 128.9 (C-5), 116.7 (C-4a), 116.2 (C-8), 42.8 (C-1′), 29.3 (C-2′), 21.0 (Ar—CH_3), 20.1 (C-3′), 14.1 (C-4′); ESI-MS (m/z): 245.1 [M−H]$^-$ (negative mode) for MW = 246.31.

*2.4.2. 3-Benzyl-2-hydrazinyl-6-methylquinazolin-4(3H)-one (**25**)*

White amorphous powder; yield: 62%; mp: 200–201 °C; ^{1}H NMR (500 MHz, DMSO-d_6) δ (ppm): 8.28 (s, 1H, —NH—), 7.77 (br s, 1H, H-5), 7.47 (br d, J = 8 Hz, 1H, H-7), 7.35–7.22 (m, 6H, H-2′-6′, 8), 5.25 (s, 2H, H-7′), 4.41 (br s, 2H, —NH_2), 2.45 (s, 3H, Ar—CH_3); ^{13}C NMR (125 MHz, DMSO-d_6) δ (ppm): 162.0 (C-4), 152.2 (C-2), 136.8 (C-4b), 136.6 (C-6), 136.4 (C-1′), 136.2 (C-7), 130.8 (C-6), 128.9 (C-5), 128.8 (C-3′/5′), 127.2 (C-2′/6′), 126.5 (C-4′), 116.6 (C-4a), 116.1 (C-8), 43.9 (C-7′), 20.9 (Ar—CH_3); ESI-MS (m/z): 279.1 [M−H]$^-$ (negative mode) for MW = 280.33.

*2.5. Preparation of 4-butyl-7-methyl-[1,2,4]triazolo[4,3-a]quinazolin-5(4H)-one (**26**)*

A mixture of compound **24** (1 mmol) and dimethyl-*N*-cyanoimidodithiocarbonate (1 mmol) in DMF (8 mL) was refluxed in the presence of Et_3N for 4 h. The mixture was then poured into ice water, and the resulting solid was separated, washed with water, and dried. Alternatively, compound **24** (1 mmol) was refluxed with formic acid (5 mL) for 7 h. The mixture was cooled, and the resulting solid was separated and dried. White amorphous powder; yield: 41%; mp: 183–184 °C; ^{1}H NMR (500 MHz, DMSO-d_6) δ (ppm): 9.46 (s, 1H, —N—C<u>H</u>=N—), 8.07 (d, J = 8.5 Hz, 1H, H-8), 8.00 (br s, 1H, H-5), 7.76 (br d, J = 8 Hz, 1H, H-7), 4.19 (t, J = 7.5 Hz, 2H, H-1′), 2.46 (s, 3H, Ar—CH_3), 1.74 (quintuplet, J = 7.5 Hz, 2H, H-2′), 1.38 (m, 2H, H-3′), 0.95 (t, J = 7.5 Hz, 3H, H-4′); ^{13}C NMR (125 MHz, DMSO-d_6) δ (ppm): 158.7 (C-4), 147.8 (C-2), 137.0 (—N—*C*H=N—), 136.2 (C-6), 136.3 (C-4b), 130.9 (C-7), 128.9 (C-5), 116.7 (C-4a), 116.3 (C-8), 42.8 (C-1′), 29.3 (C-2′), 21.0 (Ar—CH_3), 20.0 (C-3′), 14.1 (C-4′); ESI-MS (m/z): 255.1 [M−H]$^-$ (negative mode) for MW = 256.31.

2.6. Cell culture

The human breast cancer (MDA-MB231) and cervical cancer (HeLa) cells were grown in Dulbecco's modified Eagle's medium (DMEM) supplemented with 10% fetal bovine serum (FBS) and 1% penicillin (10,000 U) and streptomycin (10 mg) in 74 cm^2 flasks and incubated until 80% confluence was reached in a humidified environment of 5% CO_2/95% air at 37 °C. The cells were seeded and maintained in triplicate in a 96-well tissue culture plate at 5×10^4 cells/well in 150 μL of the growth medium for experimental purposes and allowed to attach for 24 h before treatment. The cells were then treated with the synthesized compounds (**1**–**26**) and gefitinib (standard) at 0, 1, 5, 10, 25, and 50 μM and incubated for 24 h. DMSO was used as a negative control, as all compounds were dissolved in 50% DMSO. The DMSO concentration in each well was maintained at less than 0.1%. After 24 h, the growth medium was replaced with 100 μl of serum-free medium containing MTT (3-(4,5-dimethylthiazol-2-yl)-2,5-diphenyltetrazolium bromide), 5 mg/mL) and incubated for 4 h at 5% CO_2/95% air and 37 °C. MTT, which is a yellow, water-soluble tetrazolium salt, is cleaved by mitochondrial dehydrogenases leading to the formation of the purple, water-insoluble formazan, which cannot pass through the cell membrane and therefore accumulates in healthy cells (Carmichael et al., 1987). The old medium was then discarded, and the formazan was dissolved by adding 100 μl of isopropanol. The absorbance of the 96-well plate was measured at 570 nm using a Mithras^2 LB 943 monochromator multimode reader (Berthold Technologies) against the reagent blank.

3. Results and discussion

3.1. Chemistry of the synthesized compounds

The 2-thioxo-2,3-dihydroquinazolin-4-ones **1** and **2**, were synthesized as previously described in literature (Al-Omar et al., 2004; Alafeefy et al., 2014), and their structures were confirmed via X-ray crystallography (Fig. 2a and b) (Al-Salahi et al., 2012a, 2012b). In the present study, 3-butyl-6-methyl-2-thioxo-2,3-dihy droquinazolin-4-one (**3**) was obtained successfully at a high yield of 87% by treating 2-amino-5-methylbenzoic acid with butyl isothiocyanate in the presence of Et_3N under reflux conditions (Scheme 1). The structure of compound **3** was characterized via NMR spectroscopy and unambiguously confirmed via X-ray crystallography (Fig. 2c).

In the presence of potassium carbonate, the reaction of compounds **1**–**3** with different alkyl (heteroalkyl) halides in boiling DMF smoothly afforded the expected thioethers (**4**–**23**) in 45–85% yields (Scheme 1 and Table 1). Hydrazinolysis of compounds **1** and **3** in boiling ethanol led to the formation of the corresponding 2-hydrazinyl-6-methyl-quinazolin-4-ones (**24** and **25**) with a good yield of 76% and 62%, respectively. The reaction of compound **3** with dimethyl-*N*-cyanoimidodithiocarbonate or formic acid under reflux furnished the tricyclic product (**26**) in good yield. The

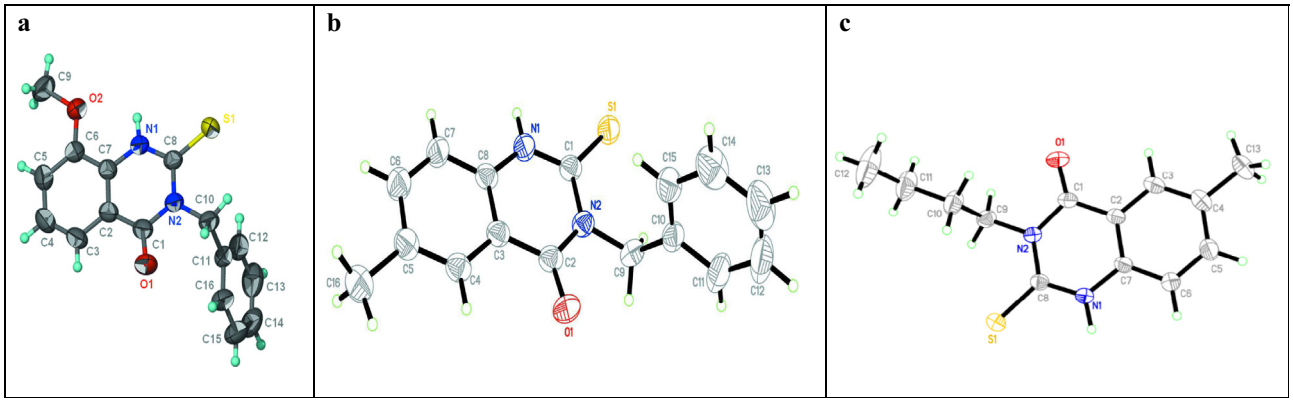

Fig. 2. Three-dimensional structures of compounds **1**–**3**.

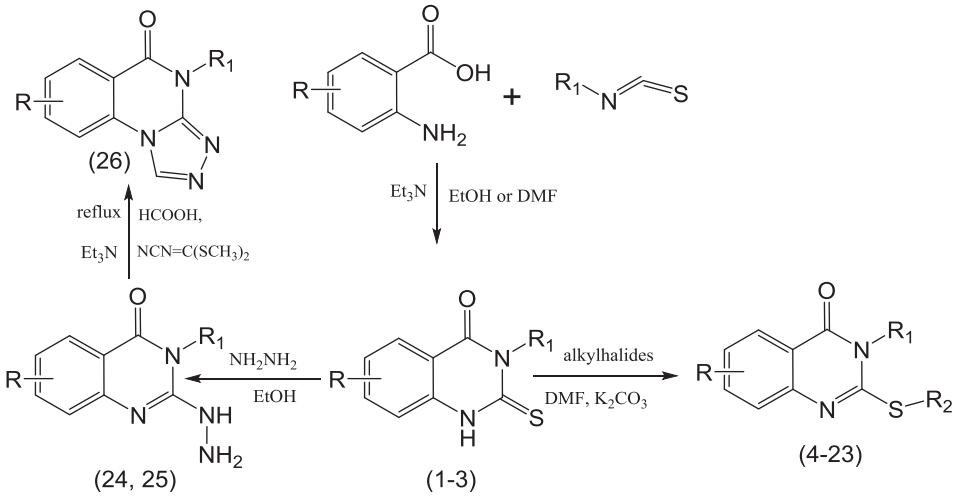

Scheme 1. The synthetic routes for compounds **1**–**26.**

thioethers (**4**–**24**), hydrazino (**24** and **25**) and tricyclic (**26**) products were obtained as pure, colored amorphous powders and their structures were confirmed via NMR analysis. The presence of the basic 2-thioxoquinazoline unit in most compounds was confirmed through its three characteristic aromatic signals of the benzene moiety observed at δ (ppm): 7.8 (br s, H-5), 7.6 (br d, H-7), and 7.5 (d, H-8). In addition, a singlet of 3H was assigned at approximately 2.45 ppm for the 6-CH_3 group, which was indicated in all the ^{13}C NMR spectra at about 21.0 ppm. Moreover, the four intrinsic ^{1}H-resonances of the *N*-butyl functional group were recorded at δ (ppm): 4.2 (t, H-1′), 1.7 (quintuplet, H-2′), 1.4 (m, H-3′), and 0.90 (t, H-4′), while their ^{13}C signals were observed at 44.0, 30.0, 20.0, and 14.0 ppm, respectively. All the ^{13}C NMR spectra of products **4**–**16** showed eight signals for the quinazoline moiety including the two key signals at 161 and 155 ppm, assignable to the C-4 carbonyl group and quaternary C-2 atom, respectively. The presence of the 2-thioxo functional group in compound **3** was confirmed by its unique carbon signal at 174.9 ppm. In the ^{1}H NMR spectrum of compound **24**, the hydrazinyl group was assigned to two broad singlets at 9.44 and 6.21 ppm that are ascribable to the —NH and —NH_2 protons, respectively. The formation of the *S*-benzyl derivatives (**6**–**13**) was also confirmed based on the observation of the —CH_2—Ar signal at 4.5–4.7 and 34–36 ppm in the ^{1}H and ^{13}C NMR spectra, respectively. Similarly, the characteristic NMR resonances of the ethyl, allyl, benzo[*d*]imidazol-2-yl, morpholinoethyl, and (phthalimido-2-yl)propyl) moieties were proof for the success-

Table 1
Synthesized quinazoline derivatives (**1**–**26**).

Compounds	R	R1	R2
1	Methyl	Benzyl	–
2	Methoxy	Benzyl	–
3	Methyl	Butyl	–
4	Methyl	Butyl	Ethyl
5	Methyl	Butyl	Allyl
6	Methyl	Butyl	2-Methyl-benzyl
7	Methyl	Butyl	3-Methyl-benzyl
8	Methyl	Butyl	4-Cl-benzyl
9	Methyl	Butyl	4-NO_2-benzyl
10	Methyl	Butyl	2-CN-benzyl
11	Methyl	Butyl	3-CN-benzyl
12	Methyl	Butyl	4-CN-benzyl
13	Methyl	Butyl	3-Methoxy-benzyl
14	Methyl	Butyl	(1*H*-benzoimidazol-2-yl)methyl
15	Methyl	Butyl	Morphilinoethyl
16	Methyl	Butyl	3-(Phthalimido-2-yl)propyl
17	Methyl	Benzyl	4-CN-benzyl
18	Methyl	Benzyl	3-Methyl-benzyl
19	Methyl	Benzyl	4-NO_2-benzyl
20	Methyl	Benzyl	7-NO_2-benzoxadiazole
21	Methyl	Benzyl	3-(Phthalimido-2-yl)propyl
22	Methoxy	Benzyl	3-(Phthalimido-2-yl)propyl
23	Methoxy	Benzyl	Morphilinoethyl
24	Methyl	Butyl	Hydrazine
25	Methyl	Benzyl	Hydrazine
26	Methyl	Butyl	–

ful preparation of their derivatives (**4**, **5**, and **14**–**16**). The products **17**–**21** and **25** showed the characteristic NMR resonances of the *N*-benzyl moiety, which comprised of —CH_2— as a singlet at 5.3 ppm in ^{1}H NMR and at about 47.0 ppm in the ^{13}C NMR spectra. They also showed three characteristic resonances of the H-5, H-7, and H-8 protons together with the typical singlet of the Ar-methyl group at 2.45 ppm and its ^{13}C signal at 21.0 ppm. In the case of compounds **22** and **23**, the methoxylated C-8 appeared at 154.0 ppm, and the methoxy-CH_3 was assigned at 3.8 ppm along with its ^{13}C signal at 57.0 ppm. Moreover, the quinazoline moiety of compounds **17**–**23** was characterized by its characteristic ^{13}C resonances, including the most downfield signals at 161.0 and 155.0 ppm that are ascribable to carbonyl C-4 and C-2, except in the case of compound **20,** in which C-2 was assigned at 159.0 ppm owing to the *S*-aryl group. In the case of compound **26**, the presence of the triazole ring was confirmed based on the appearance of its methine—H as a singlet at 9.46 ppm and its ^{13}C signal at 137.0 ppm. Finally, it is worth mentioning to refer that the structure elucidation and the confirmation of all structures was achieved through a comparison study with the corresponding NMR data of related structure compounds (Al-Salahi et al., 2013, 2014b, 2015).

3.2. Antitumor activity of the synthesized compounds

Quinazolines have previously been demonstrated to be potent anticancer agents that are suitable for inhibiting EGFR-TKs (Arteaga and Johnson, 2001; Barlési et al., 2005; Alafeefy et al., 2014, 2015; Tiwari et al., 2015; El-Messery et al., 2016). Thus, the present study focused on evaluating the cytotoxicity of compounds **3**–**26** and comparing it with that of the parents (**1** and **2**). The *in vitro* cytotoxicity of the target compounds (**1**–**26)** was evaluated against the HeLa and MDA-MB231 carcinoma cell lines using gefitinib as a standard. The inhibition of cell proliferation was measured using the MTT assay (Carmichael et al., 1987). Each cell line was incubated with six different concentrations (0–50 μM) of each compound, and the compound concentration versus survival fraction curves were created. The IC_{50} values of compounds **1**–**26** are shown in Table 2. The cytotoxicity of all tested compounds (IC_{50} = 2.3–6.1 μM), with the exception of compound **11** (IC_{50} = 95.97 μM), against the MDA-MB231 cell line was higher than that of gefitinib (IC_{50} = 28.33 μM), with compound **15** showing good effectiveness (IC_{50} = 17.57 μM). Similarly, compounds **2**, **3, 8**, **10**, **17**, **18,** and **21**–**23** were more potent (IC_{50} = 1.85–3.9 μM) than gefitinib (IC_{50} = 4.3 μM) against the HeLa cell line. However, compounds **4**–**7**, **9**, **11, 15**, **16**, **19**, **20**, and **24**–**26** demonstrated good cytotoxicity against the HeLa cell line (IC_{50} = 4.1–6.3 μM), compounds **1** and **12**–**14** exhibited moderate activity (IC_{50} = 6.7–10.63 μM). The antitumor activity of the tested quinazoline derivatives (**1**–**26**) against the HeLa and MDA-MB231 cancer cell lines followed a distinctive pattern with compounds **21**–**23** exhibiting the most potent activity against both cell lines in this study. The anticancer activity of compounds **1**–**26** against HeLa and MDA-MB231 cells could be correlated with their structural modifications. An investigation of the diversity in the selectivity of compounds **1**–**26** for the two cell lines revealed that most of the tested compounds significantly inhibited both cell lines.

The parents **1**–**3** exhibited remarkable activity against HeLa and MDA-MB231 cells (Table 2). However, compound **2** (IC_{50} = 2.7 μM) was more potent than compounds **1** and **3** (IC_{50} = 10.63 and 3.73 μM, respectively) against the HeLa cell line, indicating that the presence of an electro-donating group (OCH_3) in compound **2** was essential for its activity. Compound **3** (IC_{50} = 2.73 μM) was more potent than compounds **1** and **2** (IC_{50} = 3.2 and 4.85 μM) against the MDA-MB231 carcinoma cell line. In this case, compound **3** showed higher activity against the MDA-MB231 cell line in relation to compound **2**, and against both cancer cell lines with respect to compound **1**. The increase in the cytotoxicity of compound **3** may be due to the presence of a highly lipophilic group (butyl) that enhances its activity.

Table 2
Anticancer activity of the target compounds (**1**–**26**) (IC_{50}, μM).

Compounds	HeLa/IC_{50}, μM	MDA-MB231/IC_{50}, μM
1	10.63	3.2
2	2.7	4.85
3	3.73	2.73
4	4.14	3.8
5	5.65	3.77
6	6.3	4.44
7	4.45	5
8	3.7	4.13
9	4.56	4.12
10	3.7	4.26
11	6.1	95.97
12	7.5	5.1
13	6.79	5.18
14	7.8	4.97
15	4.11	17.57
16	5.75	6.19
17	3.9	2.93
18	3.04	4.96
19	5.6	3.23
20	4.14	3.5
21	1.85	2.33
22	2.5	2.56
23	2.6	2.81
24	5.39	2.74
25	4.77	5.6
26	5.03	5.74
Gefitinib	4.3	28.33

The type of substituent incorporated at position 2 in compounds **1**–**3** was also found to be a major determinant of the cytotoxicity. Accordingly, the cytotoxicity increased in the order of **4, 5** > **6**–**16** and **3**, **10** > **4**–**9**, **11**–**16** against the MDA-MB231 and HeLa cell lines, respectively, in relation to compound **3** and gefitinib. The cytotoxicity profile was also affected by the variation and configuration of substituents on the *S*-benzyl ring, which was indicated by the increase in the anticancer activity of compounds **10**–**12** that contain the CN group, with compound **10** (IC_{50} = 3.7 and 4.26 μM) showing the highest activity. This indicates that the presence of the CN group in the *ortho* position enhanced the activity. Although the presence of a methoxy group in compound **13** did not enhance its cytotoxicity in comparison to compound **3,** it was beneficial for improving the efficacy of the parent molecule **2**. Incorporation of heteroalkyl groups into compound **3** afforded compounds **14**–**16** with slightly decreased cytotoxicity. Conversely, compounds **21**–**23** showed the highest activity against both carcinoma cell lines, and compounds **17** and **19** were more potent than compounds **9** and **12** against both cell lines. An explanation for this is that the presence of phthalimido, morpholino, NO_2, and CN groups alongside the *N*-benzyl group might play a substantial role in the cytotoxicity and selectivity of these compounds. Hydrazinolysis of compounds **1** and **3** into compounds **24** and **25** influenced positively in the case of compounds **1** (IC_{50} = 4.77 μM) and **3** (IC_{50} = 2.74 μM) against the HeLa and MDA-MB231 cell line, respectively. The incorporation of a triazole ring in compound **26** caused a slight decrease in cytotoxicity. These variations in the anticancer activity profile of compounds **1**–**26** could also be correlated with the differences in the lipophilic substitution pattern of the quinazoline core.

4. Conclusion

Our results indicated that all tested compounds (**1**–**26**) showed good activity against the HeLa and MDA-MB231 cancer cell lines.

In particular, compounds **21**–**23**, which had the lowest IC_{50} values in relation to gefitinib, were identified as the most potent agents that probably act via the EGFR-TK pathway.

The obtained remarkable and significant cytotoxicity effects of compounds **21**–**23** (IC_{50} range of 1.85–2.81 μM) using aromatic and hetero substituent of the quinazoline core could be considered as useful template for future design and further derivatization or modification to obtain more compounds with potent cytotoxic effects.

Conflict of interest

The authors declare no potential conflicts of interest with respect to the research, authorship, and publication of this article.

Acknowledgements

The authors extend their appreciation to the Deanship of Scientific Research at King Saud University for funding this work through the research group project no. RG-1435-068.

References

Alafeefy, A.M., Ceruso, M., Al-Tamimi, A.M.S., Del Prete, S., Capasso, C., Supuran, C.T., 2014. Quinazoline-sulfonamides with potent inhibitory activity against the α-carbonic anhydrase from *Vibrio cholera*. Bioorg. Med. Chem. 22, 5133–5140.

Alafeefy, A.M., Ceruso, M., Al-Jaber, N.A., Parkkila, S., Vermelho, A.B., Supuran, C.T., 2015. A new class of quinazoline-sulfonamides acting as efficient inhibitors against the α-carbonic anhydrase from *Trypanosoma cruzi*. J. Enzyme Inhib. Med. Chem. 30, 581–585.

Al-Omar, M.A., Abdel-Hamide, S.G., Al-Khamees, H.A., El-Subbagh, H.I., 2004. Synthesis and biological screening of some new substituted-3*H*-quinazolin-4-one analogs as antimicrobial agents. Saudi Pharm. J. 12, 63–71.

Al-Rashood, S.T., Aboldahab, I.A., Nagi, M.N., Abouzeid, L.A., Abdel-Aziz, A.A.M., Abdel-Hamide, S.G., Youssef, K.M., Al-Obaid, A.M., El-Subbagh, H.I., 2006. Synthesis, dihydrofolate reductase inhibition, antitumor testing, and molecular modeling study of some new 4(3*H*)-quinazolinone analogs. Bioorg. Med. Chem. 14, 8608–8621.

Al-Salahi, R., Al-Omar, M., El-Subbagh, H., Hemamalini, M., Fun, H.K., 2012a. 3-benzyl-6-methyl-2-sulfanylidene-2,3-dihydroquinazoline-4(1*H*)-one. Acta Crystallogr. Sect. E: Struct. Rep. Online 68, o717–o718.

Al-Salahi, R., Al-Omar, M., Marzouk, M., Ng, S.W., 2012b. 3-benzyl-8-methoxy-2-sulfanylidene-1,2,3,4-tetrahydroquinazolin-4-one. Acta Crystallogr. Sect. E: Struct. Rep. Online 68, o1807–o1813.

Al-Salahi, R., Alswiadan, I., Al-Omar, M., Marzouk, M., 2013. Synthesis and antimicrobial of new 2-Phenoxy-4*H*-[1,2,4]triazolo[1,5-*a*]quinazoline derivatives. Life Sci. J. 10, 2018–2028.

Al-Salahi, R., Alswaidan, I., Marzouk, M., 2014a. Cytotoxicity evaluation of a new set of 2-aminobenzo[*de*]iso-quinoline-1,3-diones. Int. J. Mol. Sci. 15, 22483–22491.

Al-Salahi, R., Tahir, K.E., Lolak, N., Hamidaddin, M., Alswaidan, I., Marzouk, M., 2014b. Biological effects of a new set 1,2,4-triazolo[1,5-*a*]quinazolines on heart rate and blood pressure. Chem. Cent. J. 8, 3.

Al-Salahi, R., El Dib, R.A., Marzouk, M., 2015. Synthesis and in vitro cytotoxicity evaluation of new 2-thioxo-benzo[*g*]quinazolin-4(3*H*)-one derivatives. Heterocycles 91, 1735–1751.

Al-Suwaidan, I.A., Abdel-Aziz, A.A.M., Shawer, T.Z., Ayyad, R.R., Alanazi, A.M., El-Morsy, A.M., Mohamed, M.A., Abdel-Aziz, N.I., El-Sayed, M.A.A., El-Azab, A.S., 2016. Synthesis, antitumor activity and molecular docking study of some novel 3-benzyl-4(3*H*)quinazolinone analogues. J. Enzyme Inhib. Med. Chem. 31, 78–89.

Ang, K.K., Andratschke, N.H., Milas, L., 2004. Epidermal growth factor receptor and response of head-and-neck carcinoma to therapy. Int. J. Radiat. Oncol. Biol. Phys. 58, 959–965.

Arteaga, C.L., Johnson, D.H., 2001. Tyrosine kinase inhibitors-ZD1839 (Iressa). Curr. Opin. Oncol. 13, 491–498.

Barker, A.J., Gibson, K.H., Grundy, W., Godfrey, A.A., Barlow, J.J., Healy, M.P., Woodburn, J.R., Ashton, S.E., Curry, B.J., Scarlett, L., Henthorn, L., Richards, L., 2001. Studies leading to the identification of ZD1839 (Iressa™): an orally active, selective epidermal growth factor receptor tyrosine kinase inhibitor targeted to the treatment of cancer. Bioorg. Med. Chem. Lett. 11, 1911–1914.

Barker, A.J., Johnstone, C., 1997. Preparation of 4-anilino-7-heteroarylquinazolines as tyrosine kinase inhibitors. WO 97/30044 A1.

Barlési, F., Tchouhadjian, C., Doddoli, C., Villani, P., Greillier, L., Kleisbauer, J.P., Thomas, P., Astoul, P., 2005. Gefitinib (ZD1839, Iressa®) in non-small-cell lung cancer: a review of clinical trials from a daily practice perspective. Fundam. Clin. Pharmacol. 19, 385–393.

Carmichael, J., DeGraff, W.G., Gazdar, A.F., Minna, J.D., Mitchell, J.B., 1987. Evaluation of a tetrazolium-based semiautomated colorimetric assay: assessment of chemosensitivity testing. Cancer Res. 47, 936–942.

Chandregowda, V., Kush, A.K., Reddy, G.C., 2009. Synthesis and in vitro antitumor activities of novel 4-anilinoquinazoline derivatives. Eur. J. Med. Chem. 44, 3046–3055.

El-Azab, A.S., Al-Omar, M.A., Abdel-Aziz, A.A.M., Abdel-Aziz, N.I., El-Sayed, M.A.A., Aleisa, A.M., Sayed-Ahmed, M.M., Abdel-Hamide, S.G., 2010. Design, synthesis and biological evaluation of novel quinazoline derivatives as potential antitumor agents: molecular docking study. Eur. J. Med. Chem. 45, 4188–4198.

El-Messery, S.M., Hassan, G.S., Al-Omary, F.A.M., El-Subbagh, H.I., 2012. Substituted thiazoles VI. Synthesis and antitumor activity of new 2-acetamido- and 2 or 3-propanamido-thiazole analogs. Eur. J. Med. Chem. 54, 615–625.

El-Messery, S.M., Hassan, G.S., Nagi, M.N., Habib, E.S.E., Al-Rashood, S.T., El-Subbagh, H.I., 2016. Synthesis, biological evaluation and molecular modeling study of some new methoxylated 2-benzylthio-quinazoline-4(3*H*)-ones as nonclassical antifolates. Bioorg. Med. Chem. Lett. 26, 4815–4823.

Fricker, J., 2006. Tyrosine kinase inhibitors: the next generation. Lancet Oncol. 7, 621.

Fukui, T., Otani, S., Hataishi, R., Jiang, S.X., Nishii, Y., Igawa, S., Mitsufuji, H., Kubota, M., Katagiri, M., Masuda, N., 2010. Successful rechallenge with erlotinib in a patient with EGFR-mutant lung adenocarcinoma who developed gefitinib-related interstitial lung disease. Cancer Chemother. Pharmacol. 65, 803–806.

Garofalo, S., Rosa, R., Bianco, R., Tortora, G., 2008. EGFR-targeting agents in oncology. Expert Opin. Ther. Pat. 18, 889–901.

Hynes, N.E., Lane, H.A., 2005. ERBB receptors and cancer: the complexity of targeted inhibitors. Nat. Rev. Cancer 5, 341–354.

Lynch, T.J., Bell, D.W., Sordella, R., Gurubhagavatula, S., Okimoto, R.A., Brannigan, B. W., Harris, P.L., Haserlat, S.M., Supko, J.G., Haluska, F.G., Louis, D.N., Christiani, D. C., Settleman, J., Haber, D.A., 2004. Activating mutations in the epidermal growth factor receptor underlying responsiveness of non-small-cell lung cancer to gefitinib. N. Engl. J. Med. 350, 2129–2139.

Meert, A.P., Martin, B., Paesmans, M., Berghmans, T., Mascaux, C., Verdebout, J.M., Delmotte, P., Lafitte, J.J., Sculier, J.P., 2003. The role of HER-2/neu expression on the survival of patients with lung cancer: a systematic review of the literature. Br. J. Cancer 89, 959–965.

Tiwari, S.K., Sachan, S., Mishra, A., Tiwari, S., Pandey, V., 2015. The anticancer activity of some novel 4-anilino quinazoline derivatives as tyrosine kinase (EGFR) inhibitor and the quantitative structure activity relationships. Int. J. Pharm. Life Sci. 6, 4819–4828.